Control of Replication Origin Density and Firing Time in Xenopus Egg Extracts

Kathrin Marheineke, Olivier Hyrien

THE JOURNAL OF BIOLOGICAL CHEMISTRY
Vol. 279, No. 27, Issue of July 2, pp. 28071–28081, 2004
Printed in U.S.A.

Control of Replication Origin Density and Firing Time in *Xenopus* Egg Extracts

ROLE OF A CAFFEINE-SENSITIVE, ATR-DEPENDENT CHECKPOINT*

Received for publication, February 12, 2004, and in revised form, April 27, 2004
Published, JBC Papers in Press, April 28, 2004, DOI 10.1074/jbc.M401574200

Kathrin Marheineke and Olivier Hyrien‡

From the Laboratoire de Génétique Moléculaire, UMR 8541, Ecole Normale Supérieure, 46 rue d'Ulm, 75230 Paris Cedex 05, France

A strict control of replication origin density and firing time is essential to chromosomal stability. Replication origins in early frog embryos are located at apparently random sequences, are spaced at close (~10-kb) intervals, and are activated in clusters that fire at different times throughout a very brief S phase. Using molecular combing of DNA from sperm nuclei replicating in *Xenopus* egg extracts, we show that the temporal order of origin firing can be modulated by the nucleocytoplasmic ratio and the checkpoint-abrogating agent caffeine in the absence of external challenge. Increasing the concentration of nuclei in the extract increases S phase length. Contrary to a previous interpretation, this does not result from a change in local origin spacing but from a spreading of the time over which distinct origin clusters fire and from a decrease in replication fork velocity. Caffeine addition or ATR inhibition with a specific neutralizing antibody increases origin firing early in S phase, suggesting that a checkpoint controls the time of origin firing during unperturbed S phase. Furthermore, fork progression is impaired when excess forks are assembled after caffeine treatment. We also show that caffeine allows more early origin firing with low levels of aphidicolin treatment but not higher levels. We propose that a caffeine-sensitive, ATR-dependent checkpoint adjusts the frequency of initiation to the supply of replication factors and optimizes fork density for safe and efficient chromosomal replication during normal S phase.

A strict control of replication origin density and time of activation is required to ensure that no DNA stretch is left unreplicated at the end of S phase. Replication initiation is governed by a conserved pathway of protein interactions at DNA replication origins (1). During late mitosis and the G_1 phase, prereplicative complexes are formed at sites defined by ORC, a six-subunit protein complex that directs the loading of other prereplicative complex components, including Cdc6, Cdt1, and the Mcm2-7 complex (2–5). After the G_1/S transition, the prereplicative complex is converted to a preinitiation complex. This process is triggered by at least two kinases, Cdc7/Dbf4 and the S-cyclin-dependent kinases, and involves the ordered binding of numerous factors that ultimately unwind origin DNA and recruit DNA polymerases (6, 7).

In early *Xenopus* embryos, S phase is very brief (~20 min), and replication initiates without sequence specificity and at close intervals (~10 kb) (8). Site-specific initiation is only detected after the midblastula transition (MBT),[1] when transcription resumes (9). Replicon size increases slightly at the MBT and more significantly at later stages (9, 10). The mechanisms regulating these changes are unknown, but one clue is that the MBT occurs after a critical number of nuclei accumulate in the embryo (11).

A completely random distribution of origins would generate some unacceptably large interorigin distances in the early *Xenopus* embryo (12). To understand the mechanisms that ensure complete chromosome replication, we and others have studied the distribution of initiation events on single DNA molecules of plasmid and sperm nuclei replicating in egg extracts (13–17). We found that replication initiates throughout S phase and at broadly distributed rather than strictly regular intervals, that interference between adjacent origins occurs, and that the frequency of initiation increases throughout S phase. We suggested that abundant potential origins may be defined by multiple Mcm complexes spread away from ORC rather than by ORC itself (13), so that a choice of which origins actually fire may occur during S phase to ensure an adequate distribution of initiation events (for a review, see Ref. 16). Indeed, Mcms bind DNA and initiate replication over a large region distant from ORC in egg extracts (18, 19).

The mechanisms that control origin firing timing are still unclear. In budding yeast, where specific origins fire at specific times, the temporal program is established during the G_1 phase (20), and three kinases, Cdk1-Clb5, Mec1, and Rad53, seem implicated in its execution during S phase. Cdk1-Clb6 only activates early origins, whereas Cdk1-Clb5 activates both early and late origins (21). A Mec1/Rad53-dependent checkpoint prevents the firing of late origins in the presence of stalled forks or DNA damage (22, 23). Interestingly, the Mec1/Rad53 pathway may also regulate origin firing time during unperturbed cell growth (23, 24). In animal cells, a correlation between replication timing, gene expression, and chromatin structure has long been observed (25, 26). The replication timing is established early in G_1 phase when chromatin is repositioned in the nucleus after mitosis (27), and an intra-S checkpoint controls the timely assembly and disassembly of replication factories under conditions of replicational stress (28).

In early *Xenopus* embryos, the lack of G_1 phase, gene expression, and euchromatin/heterochromatin differentiation raises questions regarding the regulation and functional role of origin firing timing. We have previously shown by DNA combing that

* This work was supported by the Ligue Nationale Française Contre le Cancer (Comité de Paris) and the Association pour la Recherche sur le Cancer. The costs of publication of this article were defrayed in part by the payment of page charges. This article must therefore be hereby marked "*advertisement*" in accordance with 18 U.S.C. Section 1734 solely to indicate this fact.

‡ To whom correspondence should be addressed. Tel.: 33-1-4432-3920; Fax: 33-1-4432-3941; E-mail: hyrien@wotan.ens.fr.

[1] The abbreviations used are: MBT, midblastula transition; Pipes, 1,4-piperazinediethanesulfonic acid.

an intra S checkpoint regulates origin firing when sperm nuclei in egg extracts are challenged with aphidicolin, a DNA polymerase inhibitor (15). We suggested that a checkpoint monitors the density of forks and regulates initiation to control the rate of DNA replication independently of the position of initiation events. Walter and Newport (29) reported that when the concentration of sperm nuclei in egg extracts exceeds the concentration of cells in a *Xenopus* MBT embryo, the length of S phase increases, although the rate of replication fork movement appears unchanged. This might be due to an increase in replicon size, possibly by depletion of an initiation factor, or to staggered initiation at individual origins. The latter hypothesis was dismissed because the addition of the cyclin-dependent kinase inhibitor p21Cip1 after the start of S phase had little effect on subsequent replication (29). However, it has since been clearly established that origins fire at different times through S phase in egg extracts (13–17).

In this paper, we use molecular combing of DNA from sperm nuclei replicating in *Xenopus* egg extracts to directly examine the effect of the nucleocytoplasmic ratio and caffeine on the pattern of origin firing. Caffeine is a potent small molecule inhibitor of the kinase activity of the Mec1 homologs ATM and ATR *in vitro* (30) and abrogates checkpoints *in vivo* (31, 32). We demonstrate that the longer S phase at high concentrations of nuclei is not due to a change in replicon size but to an expansion of the period of time over which origins fire and to a lower replication fork velocity. Treatment with caffeine increases origin firing but decreases fork velocity. Inhibition of ATR with a specific neutralizing antibody also increases origin firing. These results suggest that an intra-S checkpoint decreases origin firing in response to a limiting factor to ensure optimal fork progression.

EXPERIMENTAL PROCEDURES

Replication of Sperm Nuclei in Xenopus Egg Extracts—Replication-competent extracts from unfertilized *Xenopus* eggs were prepared as described (33) and used fresh. Sperm nuclei (100–6000 nuclei/μl) were incubated in extracts in the presence of cycloheximide (250 μg/ml), energy mix (7.5 mM creatine phosphate, 1 mM ATP, 0.1 mM EGTA, pH 7.7, 1 mM $MgCl_2$), 20 μM digoxigenin-dUTP (added at $t = 0$), and 20 μM biotin-dUTP (added at the indicated times) (Roche Applied Science). Replication was allowed to continue for 2 h. Aphidicolin block-and-release experiments were performed as described previously (15). Caffeine (or buffer alone as control) was added where indicated to a final concentration of 5 mM from a 100 mM solution freshly dissolved in 10 mM Pipes-NaOH, pH 7.4. ATR-neutralizing antibodies (34) were added where indicated.

Molecular Combing and Detection by Fluorescent Antibodies—DNA was extracted and combed as described (14, 15). Biotin was detected with Texas Red-conjugated antibodies (15). For the digoxigenin label, a mouse fluorescein isothiocyanate-conjugated anti-digoxigenin antibody was used followed by Alexa Fluor 488 rabbit anti-mouse and goat anti-rabbit antibodies (Molecular Probes, Inc., Eugene, OR) for enhancement.

Measurements and Data Analysis—Images of the combed DNA molecules were acquired and measured as described (15). Fields of view were chosen at random in the fluorescein isothiocyanate channel and then photographed under the fluorescein isothiocyanate and the Texas Red filter. The size of most photographed molecules was 120 kb. All photographed fibers showed a continuous digoxigenin label, indicating complete replication. Replication eyes, gaps, and forks were defined as described under "Results." Tracts of biotin-negative DNA needed to be >2 kb to be considered significant and scored as eyes.

The replication extent of each fiber (or group of fibers) was defined as the sum of eye lengths divided by the total length of the molecule(s). Fork density is the total number of forks divided by total DNA length (kb) in each sample. The overall mean eye length and gap length were determined by dividing the total replicated or unreplicated length, respectively, by half the number of forks in each sample. Similarly, the overall mean eye-to-eye distance was determined by dividing the total DNA length by half the number of forks. Note that this is just twice the inverse of fork density. These numbers are not affected by the finite size of the analyzed molecules. However, to analyze the distribution of eye lengths, gap lengths, and eye-to-eye distances, incomplete eyes or gaps located on either end of each fiber had to be excluded. This bias resulted in a difference between "local" measurements and "overall" means calculated as above. Therefore, the mean value of "excluded" eye lengths, gap lengths, and eye-to-eye distances were also calculated by dividing the total excluded length of replicated, unreplicated, or total DNA, respectively, by half the number of excluded forks.

The average fork velocity (kb/min) between two successive time points was calculated as the difference in replication extent between the two time points divided by the average fork density (number of forks/kb of total DNA) and by the time interval (min). The average fork density is defined as the mean of the fork density at the two time points. Small errors can therefore result if the change in fork density between the two time points is not linear. We also caution that with eyes of <2 kb being excluded from analysis, velocities may be slightly overestimated, but this should not affect comparisons between different concentrations of nuclei at similar replication extents.

Alkaline-agarose Gel Electrophoresis—Sperm nuclei were incubated in fresh extracts added with 5 mM caffeine or buffer alone as control and one-fiftieth volume of [α-^{32}P]dATP (3000 Ci/mmol). DNA was purified, separated on 1.1% alkaline-agarose gels, and analyzed as described (15).

RESULTS

Shorter S Phase at Low Nuclei Concentration Is Due to More Synchronous Origin Firing and Faster Fork Progression—When sperm nuclei are incubated in *Xenopus* egg extracts, there is an initial lag period of ~25 min during which replication origins are assembled on DNA and replication-competent nuclei are produced. After this lag, S phase starts abruptly. Most nuclei start to replicate within ~5 min of each other. S phase is very brief (typically < 30 min), but its exact length depends on the concentration of nuclei. In order to visualize origin firing and fork progression at different nuclei concentrations, we used DNA combing, a powerful DNA spreading technique (35) that has been adapted for single molecule analysis of DNA replication (14, 15). Sperm nuclei were incubated at 100 or 2000 nuclei/μl in egg extracts supplemented with digoxigenin-dUTP, so as to label all replicated DNA. Biotin-dUTP was added at different time points after the start of replication to differentially label early and late replicating sequences. After a 2-h incubation, the DNA was purified and combed on silanized coverslips, and the two labels were detected with fluorescent antibodies as described under "Experimental Procedures" (Fig. 1*A*). This double-labeling protocol allows us to ascertain the full replication of the fiber after 2 h and the fiber continuity between successive biotin-labeled tracts. Replication eyes are defined as regions replicated before the addition of biotin-dUTP and appear as tracts of digoxigenin-positive, biotin-negative DNA. Gaps are regions replicated after biotin-dUTP addition. Forks are the transition points between biotin-labeled and unlabeled segments. Eye-to-eye distances are measured between the midpoints of adjacent eyes. Combed DNA molecules are parallel, straight, and homogeneously stretched (1 μm = 2 kb) (Fig. 1*A*). About 50–80 randomly chosen DNA fibers (5–10 Mb) were analyzed for each time point.

The replication extent (at the time of biotin-dUTP addition) of each group of fibers was defined as the sum of eye lengths divided by the total DNA length. The time required for >80% of the DNA to be replicated was shorter at 100 nuclei/μl (~10 min) than at 2000 nuclei/μl (~25 min) (Figs. 1*D* and 2*A*). This was also observed by measuring the time course of incorporation of α-^{32}P]dATP into sperm DNA (not shown). The synchrony with which individual nuclei entered S phase was only 3–5 min tighter at 100 nuclei/μl than at 2000 nuclei/μl (as estimated by incorporation of rhodamine-dUTP into individual nuclei; not shown), which is insufficient to account for the 15-min difference in replication time. Therefore, S phase was about half as long at 100 nuclei/μl as at 2000 nuclei/μl. This may result from a faster progression of replication forks, a shorter interorigin distance, or a more synchronous firing of

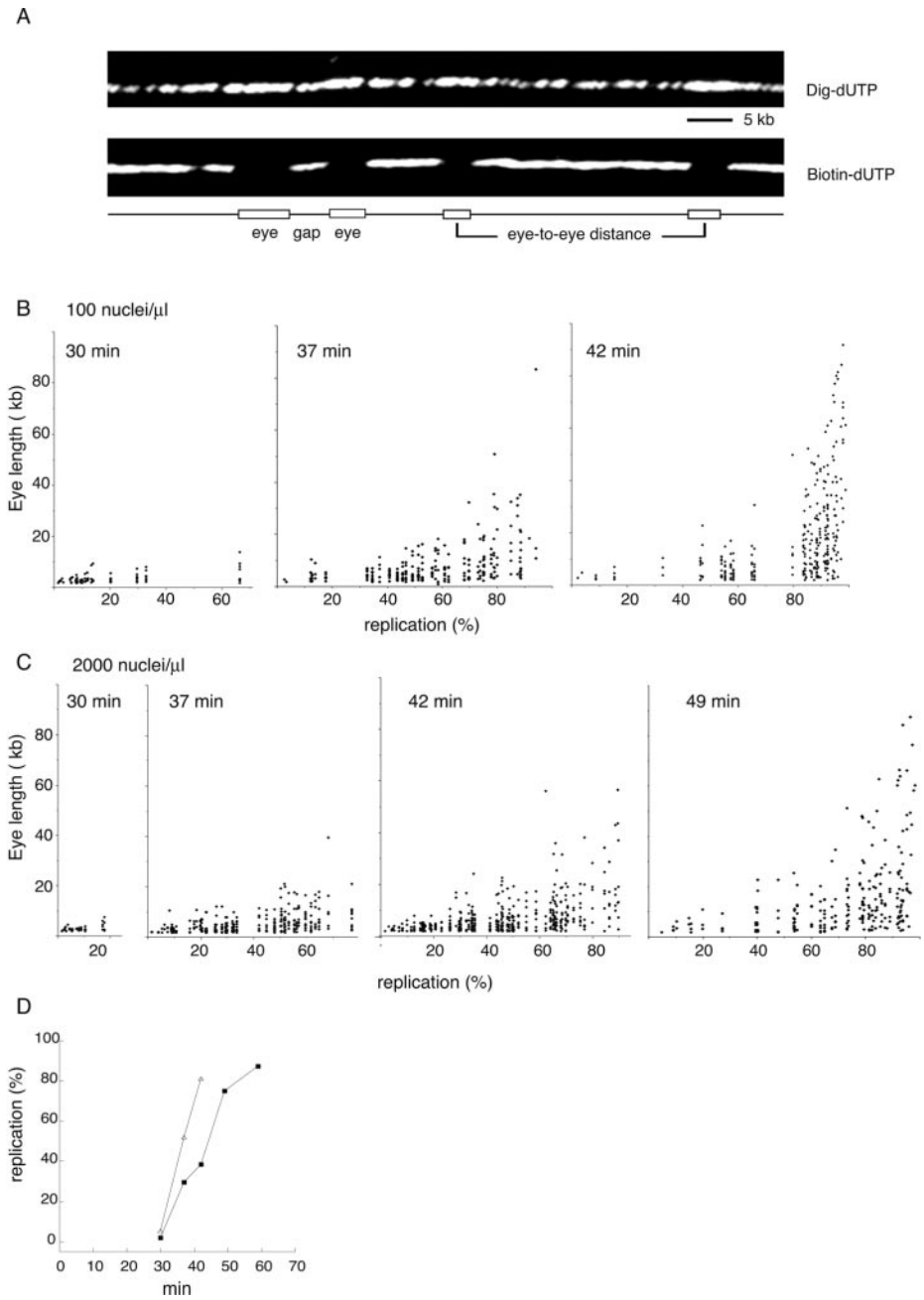

FIG. 1. **S phase progression is quicker at 100 than at 2000 nuclei/μl, but origins fire throughout S phase in both cases.** Sperm nuclei were replicated at 100 or 2000 nuclei/μl in *Xenopus* egg extracts in the presence of digoxigenin-dUTP. Biotin-dUTP was added at the indicated times, and incubation continued for 2 h. DNA was combed, and single fiber analysis was performed as described under "Experimental Procedures." *A*, an exemplary DNA fiber viewed under the fluorescein isothiocyanate (digoxigenin) and Texas Red (biotin) filters and interpretation. *B* and *C*, eye lengths of each fiber were plotted against the replication extent of the fiber for each indicated time point at 100 nuclei/μl (*B*) and at 2000 nuclei/μl (*C*). *D*, kinetics of S phase at 100 nuclei/μl (*white triangles*) and 2000 nuclei/μl (*black squares*). Eye lengths were measured on single fibers, and the percentage of replicated DNA was calculated at different time points. Incomplete eyes were included.

origins. It was shown using alkaline gel electrophoresis of nascent strands formed after release from Ara-C arrest that the rate of replication fork movement in *Xenopus* egg extracts is the same from 125 to 10,000 nuclei/μl (29). However, fork velocity might be perturbed by Ara-C treatment, which is now known to uncouple helicase from polymerase movement (6). Therefore, we used DNA combing to monitor origin activation, measure interorigin distances, and estimate fork velocity at different stages of unperturbed S phase.

Origin synchrony was assessed by determining the replication extent of each DNA fiber (sum of eye lengths divided by fiber length) and by plotting the lengths of individual eyes against the fiber's replication extent (Fig. 1, *B* and *C*). Each *vertical alignment* of *dots* in Fig. 1, *B* and *C*, thus represents the lengths of eyes of a single DNA fiber. A heterogeneous distribution of fiber replication extents and eye lengths was observed at all stages of S phase at 100 (Fig. 1*B*) and 2000 nuclei/μl (Fig. 1*C*). Small eyes, which indicate new initiation events, were visible at all time points and all replication extents. Thus, even at 100 nuclei/μl, replication origins fired continuously throughout S phase, as previously reported for plasmid DNA (13) or sperm nuclei at 2000 nuclei/μl (15). Not only did origins within a given fiber fire asynchronously, but different fibers also showed a wide distribution of replication extent at all stages of S phase. To assess whether adjacent origins fire more synchronously than pairs of origins taken at

A

Incubation time	30 min		37 min		42 min		49min	59 min
Concentration of nuclei (#/µl)	100	2000	100	2000	100	2000	2000	2000
Total DNA length (kb)	5664	6250	4592	5677	7636	8867	6167	16658
Total replicated length (kb)	364	135	2400	1704	6210	3332	4645	14695
Replication extent	6.4%	2.2%	52.3%	30.0%	81.3%	37.6%	75.3%	88.2%
Total # of fibers	47	50	40	48	62	73	51	137
Unreplicated fibers	12	31	2	3	0	2	1	0
Fully replicated fibers	0	0	0	0	5	0	3	49
Mean fiber length (kb)	120,5	125	114.8	118.3	123.2	121.5	120.9	121.6
Total # of forks	212	89	533	613	550	948	444	614
fork density (forks/kb)	1/26.7	1/70.2	1/8.6	1/9.3	1/13.9	1/9.4	1/13.9	1/27.1
Eye-to-eye distances (kb) :								
overall (total DNA length / half # of forks)	53.4	140.4	17.2	18.6	27.7	18.7	27.7	54.2
local: mean, (#)	20.6 (72)	24.7 (27)	12.6 (225)	14.2 (256)	16.8 (189)	15.3 (400)	17.0 (159)	18.7 (183)
excluded : mean, (#)	123 (34)	319 (17.5)	42.3 (41.5)	40.4 (50.5)	51.9 (86)	37.1 (74)	55.0 (63)	106.7 (124)
Eye lengths (kb) :								
overall (total repl. length / half # of forks)	3.4	3.0	9.0	5.6	22.6	7.0	20.9	47.9
local : mean, (#)	3.4 (105)	2.9 (44)	7.9 (260)	5.4 (301)	15.0 (251)	7.0 (474)	14.0 (212)	15.7 (246)
excluded : mean, (#)	3.4 (1)	15.4 (0.5)	53.2 (6.5)	14.4 (5.5)	101.9 (24)	-	167.7 (10)	182.0 (161)
Gap lengths (kb) :								
overall (total unrepl. length / half # of forks)	50.0	137.4	8.2	13.0	5.2	11.7	6.9	6.4
local : mean, (#)	17.2 (72)	21.2 (27)	5.4 (238)	8.6 (269)	3.8 (261)	8.0 (418)	4.6 (200)	5.5 (295)
excluded : mean, (#)	119.2 (34)	284.1(17.5)	31.8 (28.5)	44.8(37.5)	31.0 (14)	40.9 (53.5)	27.4 (22)	28.3 (12)

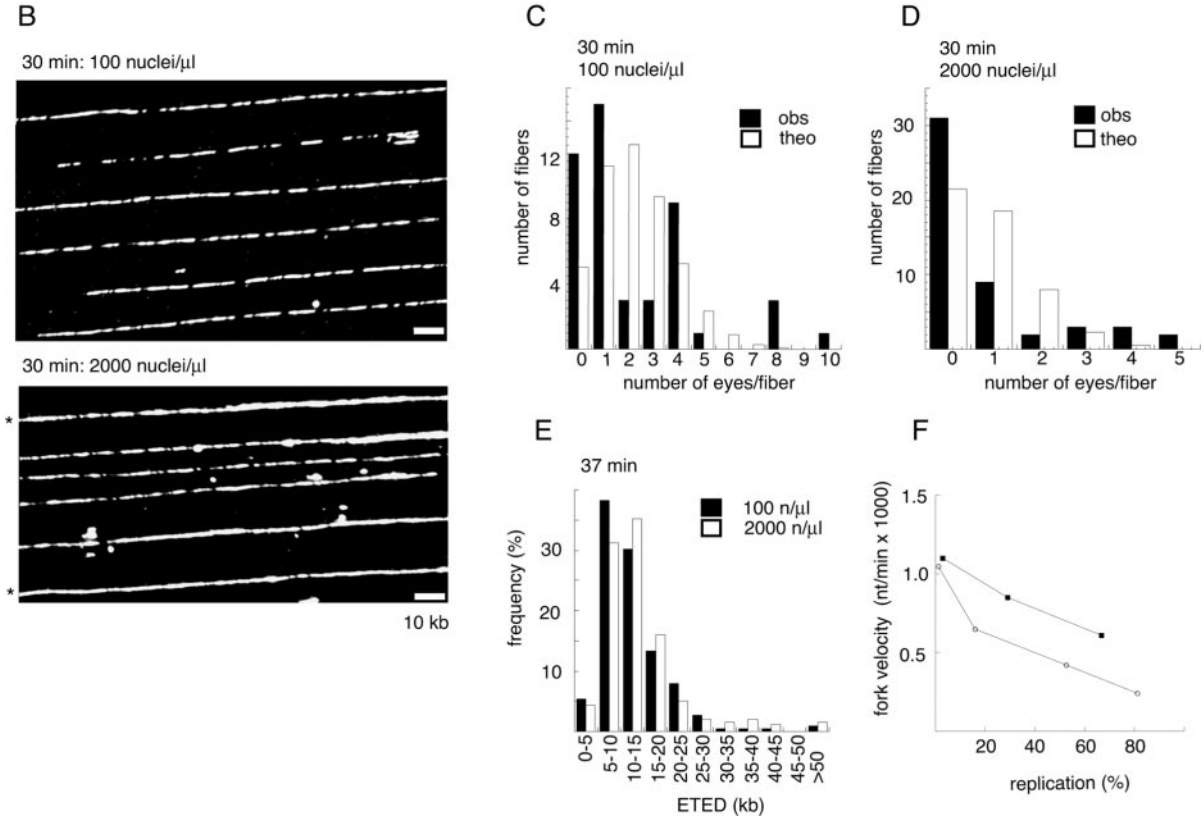

FIG. 2. **At low nuclei concentration origin clusters fire more synchronously and replication forks progress faster.** *A*, replication parameters values of combed DNA fibers for each successive time point at 100 and 2000 nuclei/µl. Definitions of overall, local, and excluded values, measurements, and calculations are described under "Experimental Procedures." *B*, representative DNA fibers labeled early in S phase (30 min) with biotin-dUTP, illustrating the different distribution of replication eyes on the fibers at 100 and 2000 nuclei/µl (*bar*, 10 kb). Unreplicated fibers are marked by *asterisks*. *C* and *D*, observed (*obs*) distributions (*black bars*) of the number of eyes per fiber at 30 min at 100 nuclei/µl (*C*) and at 2000 nuclei/µl (*D*). In each case, a theoretical (*theo*) Poisson distribution with the same mean (*white bars*) is shown for comparison. The difference between observed and Poisson distribution is highly significant at both nuclei concentrations (χ^2 test, $p < 0.001$). *E*, distribution of eye-to-eye distances (*ETED*) in mid-S phase (37 min) at 100 nuclei/µl (*black bars*) and 2000 nuclei/µl (*white bars*). *F*, average fork velocities between successive time points at 100 nuclei/µl (*black squares*) and 2000 nuclei/µl (*white circles*) are plotted against the average replication extent between the two time points.

random, the correlation coefficient between the lengths of adjacent eyes was calculated (excluding eyes >8 kb to avoid mergers). A weak but significant correlation of 0.16 was previously reported for a concentration of 3000 nuclei/µl, suggesting that origins are activated in clusters that fire at different times within S phase (17). We found similar correlations at all time points for both concentrations of nuclei (0.16–0.22; $p < 0.05$).

We then had a closer look at fibers from the 30-min time point (Fig. 2, *A* and *B*). Both samples corresponded to very early S phase (replication extent $r = 6.4\%$ at 100 nuclei/µl and 2.2% at 2000 nuclei/µl). The distributions of the number of eyes per fiber (Fig. 2, *C* and *D*, *black bars*) were non-Poissonian ($p < 0.001$), with an excess of fibers containing either no eye or multiple eyes (compare *black* and *white bars*). This confirms that at either concentration of nuclei, origins are not activated independently of each other but as clusters.

Fibers with no replication eye were 2.5-fold less frequent at 100 than at 2000 nuclei/µl (Fig. 2, *A–D*). The higher replication

extent at 100 nuclei/μl was not due to a longer eye length (mean of 3.4 *versus* 3.0 kb) but to a higher fork density (total number of forks divided by total DNA length in each sample; 1/26.7 *versus* 1/70.2 kb). Extrapolation of the replication *versus* time plots (Fig. 1*B*) to 0% replication suggests that S phase started at the same time (t ~27 min), and fork velocity was similar (~1.1 kb·min^{-1}; see "Experimental Procedures") at the two nuclei concentrations. However, 2.6-fold more origins had fired at 100 than at 2000 nuclei/μl at 30 min. This was also observed with nuclei synchronized by aphidicolin block-and-release (see below) and therefore cannot be explained by an asynchrony with which nuclei initiate replication when the concentration of nuclei increases.

Although the overall eye-to-eye distance (total DNA length divided by half the number of forks) was smaller at 100 than at 2000 nuclei/μl (53.4 *versus* 140.4 kb), the local eye-to-eye distances directly measured on individual fibers at 30 min were not markedly different (mean of 20.6 *versus* 24.7 kb) (Fig. 2*A*). This apparent discrepancy arises from the cluster organization and the limit in fiber length set by DNA breaks and/or microscope field. Incomplete eyes or gaps (and associated eye-to-eye distances) located on either fiber end are excluded from the individual measurements, and large (intercluster) distances have a greater probability to be excluded, whereas all DNA and forks are taken into account to calculate fork density (or overall eye-to-eye distance, which is twice the inverse of fork density). Importantly, it is possible to calculate the number and mean length of those excluded distances, as explained under "Experimental Procedures" (Fig. 2*A*). At 30 min, the excluded distances represented an important proportion (32 and 39%, respectively) of all eye-to-eye distances and were significantly shorter at 100 than at 2000 nuclei/μl (130 *versus* 319 kb). It is this class of distances (*i.e.* intercluster), not the local (intracluster) distances, that account for the large difference in fork density between the two samples. The analysis of gap lengths was entirely consistent with these conclusions (not further described, but see Fig. 2*A*). In summary, about 2 times more origin clusters (and 20–30% more origins per cluster) were activated at the start of S phase at 100 than at 2000 nuclei/μl.

We next focused on the 37-min time points, which correspond to mid-S phase (r = 52.3% for 100 nuclei/μl and 30.0% for 2000 nuclei/μl). The overall (17.2 *versus* 18.6 kb), local (12.6 *versus* 14.2 kb; distributions shown on Fig. 2E), and excluded (42.3 *versus* 40.4 kb) eye-to-eye distances were now similar at both concentrations of nuclei. The higher replication extent at 100 nuclei/μl was entirely explained by a longer mean eye length (9.0 *versus* 5.6 kb). The 2.15-fold higher rate of eye growth was due to a higher rate of both fork progression and eye merger. Eyes of >25 kb were ~10 times more frequent, and eyes of <5 kb were ~25% less frequent at 100 nuclei/μl than at 2000 nuclei/μl, suggesting more mergers (not shown). Although fork velocity was only 1.3-fold higher at 100 nuclei/μl than at 2000 nuclei/μl (~850 and ~650 nt·min^{-1}, respectively), replication from 30 to 37 min was 1.65-fold faster at 100 than at 2000 nuclei/μl (52.3 − 6.4 = 45.9% *versus* 30.0 − 2.2 = 27.8%). This implies that fork density increased faster at the beginning of S phase, although the same plateau was reached at 37 min (~1 fork/9 kb).

From 37 to 42 min, the fork density decreased from ~1 fork/9 kb to ~1 fork/14 kb at 100 nuclei/μl, consistent with mergers, but remained stable at ~1 fork/9 kb at 2000 nuclei/μl (Fig. 2*A*). Despite the higher average fork density at 2000 than at 100 nuclei/μl, the replication extent increased 3.8-fold less (37.6 − 30.0 = 7.6% *versus* 81.3 − 52.3 = 29.0%). The replication extent at 42 min at 2000 nuclei/μl might have been underestimated, due to some bias in the fiber sample, because the plot in Fig. 1*D* shows an unexpected inflection at this point. Nevertheless, the fork velocity was ~610 nt·min^{-1} at 100 nuclei/μl from 37 to 42 min, but only ~420 nt·min^{-1} at 2000 nuclei/μl from 37 to 49 min. These data suggest that the rate of fork progression is more variable than hitherto appreciated (Fig. 2*F*).

When replication reached >75–80%, replicon merge became predominant over new initiation. Eye-to-eye distances increased, gaps decreased, and unreplicated fibers disappeared (Fig. 2*A*). However, fully replicated fibers were still in a minority (5 of 62 and 49 of 137). Therefore, a large fraction of origin clusters was still active in late S phase.

We conclude that S phase is shorter at 100 than at 2000 nuclei/μl because (i) groups of origins that are activated sequentially at 2000 nuclei/μl fire more synchronously at 100 nuclei/μl and (ii) forks progress more rapidly at 100 nuclei/μl. Local eye-to-eye distances are almost identical, and origin clusters are still activated at different times throughout S phase but in a time frame that is compressed at 100 nuclei/μl relative to that observed at 2000 nuclei/μl. As a result, the maximum density of forks (~1/9 kb in both cases), which dictates the maximum genome replication rate, is reached faster, and replicon and cluster fusion also occur over a shorter time. In addition, fork velocity decreases as much as ~2- to ~4-fold during S phase progression.

Effect of Very High Nuclei Concentration and Synchronization by Aphidicolin Block and Release—To further explore the influence of the nuclei concentration on the control of S phase, we repeated the experiment as above at 2000 and 6000 nuclei/μl (Fig. 3). The results at 2000 nuclei/μl were consistent with the previous experiment (compare Figs. 2*A* and 3*A*). The time to replicate the DNA was 10–15 min shorter at 2000 than at 6000 nuclei/μl (Fig. 3*B*), and again this was only partly due to a tighter synchrony of S phase entry (not shown). The replication extent at 35 min was 4.2-fold higher at 2000 than at 6000 nuclei/μl (32.1 *versus* 7.6%), due to smaller overall eye-to-eye distances (24.0 *versus* 53.3 kb) and longer eyes (7.7 *versus* 4.1 kb). Fork velocities were similar at this stage (850 nt·min^{-1} *versus* 820 nt·min^{-1}). Again, the local eye-to-eye distances were not very different (Fig. 3*D*; mean of 13.9 *versus* 17.0 kb), but the excluded distances were (70.6 *versus* 158.6 kb). These data suggest that 2 times more origin clusters had fired, and more mergers had occurred at 35 min at 2000 than at 6000 nuclei/μl. This is also seen in the distributions of the number of eyes per fiber (Fig. 3*E*). The replication extent, eye-to-eye distances, and eye lengths reached at 45 min at 6000 nuclei/μl were very similar to those observed at 35 min at 2000 nuclei/μl (Fig. 3*A*), confirming that the difference in S phase length was due in large part to the time needed to reach a similar, maximal density of forks (~1 fork/11 kb in this experiment). In addition, fork velocities were 15–20% higher from 35 to 70 min at 2000 than at 6000 nuclei/μl, and there was a decrease in fork velocity during S phase (Fig. 3*C*). Only a modest proportion of fibers (32 of 59 and 37 of 82) were fully replicated when replication reached 85–90%, confirming that a large fraction of origin clusters remained active until late in S phase. In summary, the effects of increasing the nucleocytoplasmic ratio from 100 to 2000 and from 2000 to 6000 nuclei/μl were qualitatively similar.

To further exclude the possibility that these results are not simply due to a different synchrony with which nuclei enter S phase at different concentrations, we incubated nuclei at 100, 2000, or 6000 nuclei/μl in the presence of aphidicolin and released them into fresh extracts. Under these conditions, the released nuclei resume DNA replication within 1–2 min of each other (15). Nevertheless, DNA combing entirely confirmed the differences in S phase length and temporal order of origin firing

A

Incubation time	35 min		45 min		55 min		70 min		80 min
Concentration of nuclei (#/μl)	2000	6000	2000	6000	2000	6000	2000	6000	6000
Total DNA length (kb)	8950	8734	7672	8132	7347	8786	5249	7707	9894
Total replicated length (kb)	2874	666	5532	3041	6287	5637	4790	6288	8981
Replication extent	32.1%	7.6%	72.1%	37.4%	85.6%	64.2%	91.3%	81.6%	90.8%
Total # of fibers	73	73	71	70	59	72	49	65	82
Unreplicated fibers	19	30	4	11	1	0	1	1	0
Fully replicated fibers	0	0	13	1	32	4	39	22	45
Mean fiber length (kb)	122.6	119.6	108.0	116.2	124.0	122.0	107.1	122.3	120.6
Total # of forks	745	328	430	722	180	830	82	345	238
fork density (forks/kb)	1/12.0	1/26.6	1/17.8	1/11.3	1/40.8	1/10.6	1/64.0	1/22.3	1/41.6
Eye-to-eye distances (kb) :									
overall	24.0	53.3	35.7	22.5	81.6	21.2	128.0	44.7	83.1
local : mean, (#)	13.9 (306)	17.0 (122)	16.2 (136)	15.0 (287)	21.4 (54)	17.1 (307)	16.0 (31)	18.7 (118)	21.5 (61)
excluded : mean, (#)	70.6 (66.5)	158.5 (42)	69.2 (79)	51.7 (74)	171.9 (36)	32.7 (108)	475.3 (10)	100.9 (54.5)	148.0 (58)
Eye lengths (kb) :									
overall	7.7	4.1	25.7	8.4	69.9	13.6	116.8	36.5	79.3
local : mean, (#)	6.8 (344)	4.0 (164)	11.3 (176)	7.1 (346)	13.0 (74)	10.8 (381)	10.4 (35)	11.5 (146)	17.8 (100)
excluded : mean, (#)	18.8 (28.5)	-	90.9 (39)	39.0 (15)	332.8 (16)	44.8 (34)	737.7 (6)	173.9 (26)	379.0 (19)
Gap lengths (kb) :									
overall	16.3	49.2	10.0	14.1	11.8	7.6	11.2	8.2	7.6
local : mean, (#)	7.1 (334)	12.7 (122)	4.5 (183)	7.9 (319)	7.8 (83)	7.1 (377)	7.7 (38)	7.1 (158)	6.5 (105)
excluded : mean, (#)	30.8 (77)	155.2 (42)	41.1 (32)	61.2 (42)	58.9 (7)	12.4 (38)	55.4 (3)	20.5 (14.5)	16.5 (14)

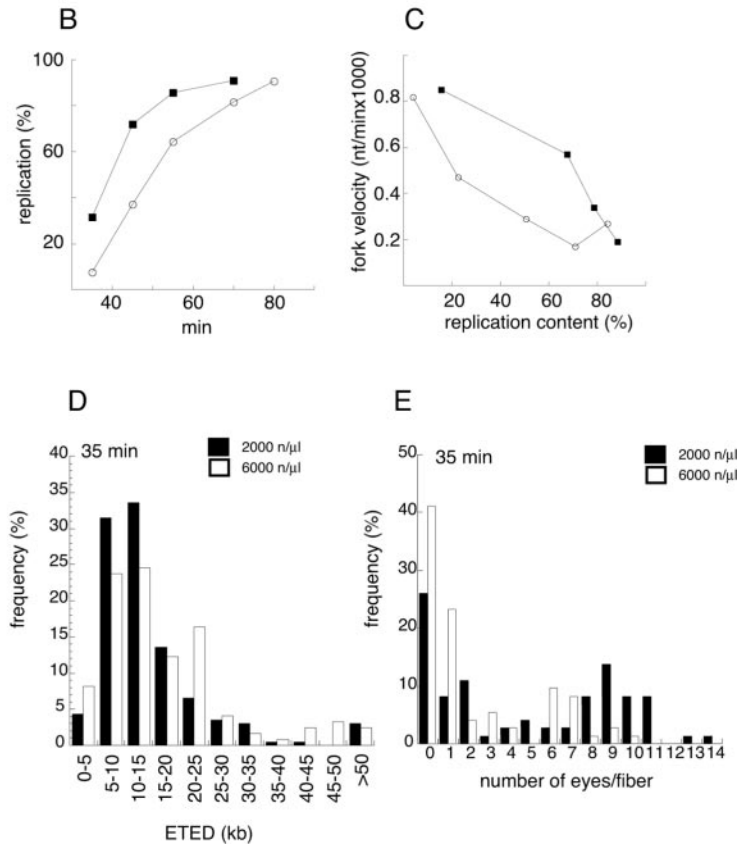

FIG. 3. **Effect of very high nuclei concentrations (6000 nuclei/μl) on S phase progression.** Sperm nuclei were replicated at 2000 or 6000 nuclei/μl in *Xenopus* egg extracts, and DNA fibers were analyzed by combing. *A*, replication parameters values for each successive time point at each nuclei concentration. *B*, kinetics of S phase at 2000 nuclei/μl (*black squares*) and 6000 nuclei/μl (*white circles*). *C* and *D*, distributions of eye-to-eye distances (*ETED*) (*C*) and number of eyes per fiber (*D*) at 35 min at 2000 nuclei/μl (*black bars*) and 6000 nuclei/μl (*white bars*). *E*, fork velocities at 2000 nuclei/μl (*black squares*) and 6000 nuclei/μl (*white circles*) were plotted against replication extent.

observed with unblocked nuclei (not shown). Fork velocity was ~250 nt·min^{-1} at all nuclei concentrations, consistent with the estimate after release from an Ara-C arrest (164 nt·min^{-1}) (29) but significantly smaller than during unperturbed S phase (see above).

Caffeine Advances the Time of Replication Origin Firing: Implication of an ATR-dependent Checkpoint—In order to investigate the role of the replication checkpoint in normal S phase progression, we preincubated egg extracts for 10 min with caffeine, an inhibitor of the ATR and ATM kinases (30–32), before adding sperm nuclei at 100 or at 2000 nuclei/μl in the presence of [α-^{32}P]dATP. The reactions were stopped at various times, and the extent of DNA replication was determined by alkaline agarose gel electrophoresis and phosphor imager quantitation (Fig 4, *A* and *B*). Caffeine increased the rate of nascent strand synthesis early in S phase by ~2–3-fold at 2000 nuclei/μl. A smaller but reproducible ~1.6-fold increase was observed at 100 nuclei/μl (not shown). Fork progression appeared unaffected at this stage, because nascent strand size profile was unchanged. We conclude that caffeine increases origin firing at the beginning of S phase, especially at high nuclei concentration.

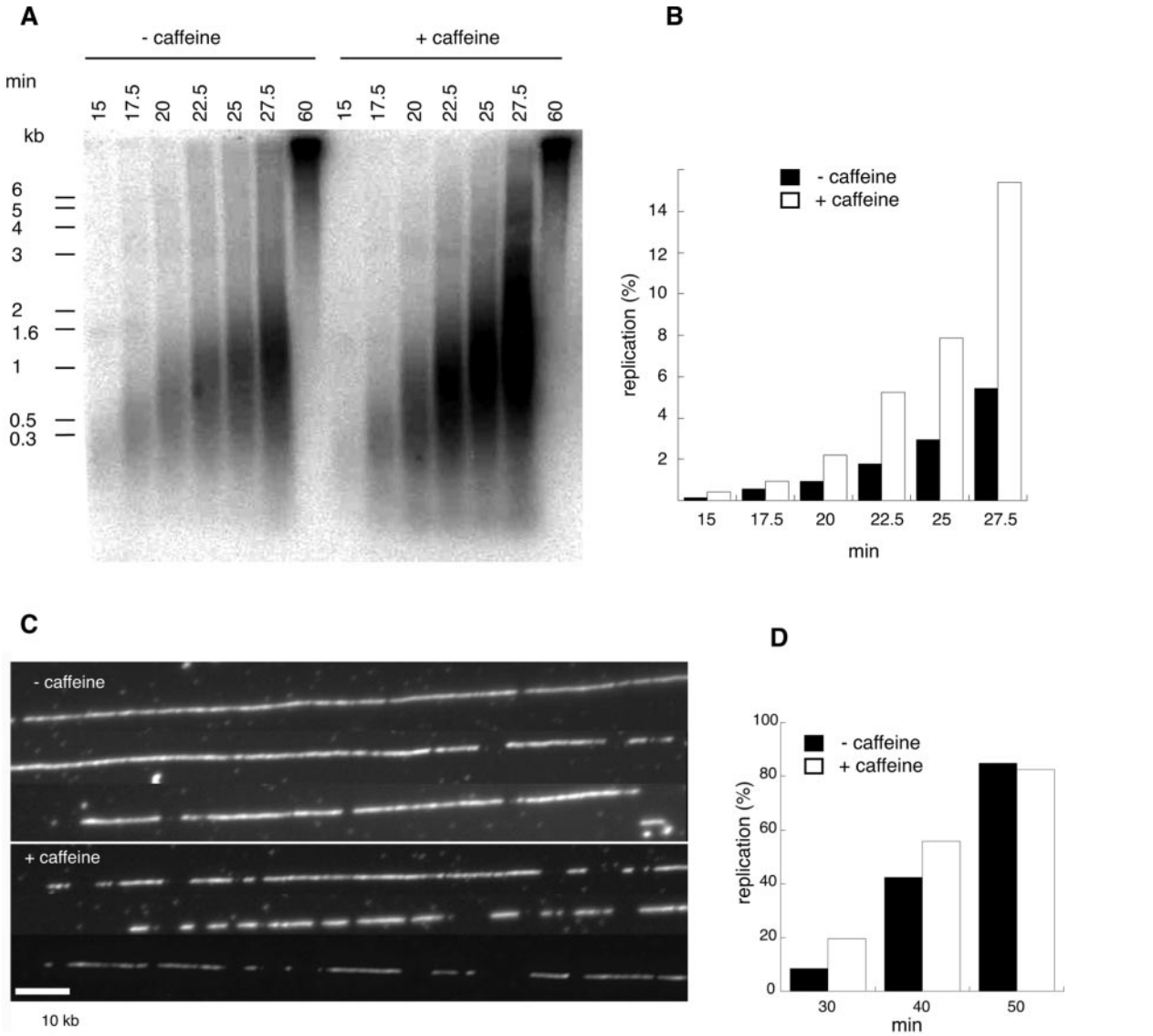

FIG. 4. **Caffeine increases origin firing in early S phase.** *A*, sperm nuclei (2000 nuclei/μl) were replicated in egg extracts in the presence of [α-^{32}P]dATP with or without 5 mM caffeine, and nascent DNA strands synthesized after the indicated times were analyzed by alkaline gel electrophoresis. *B*, quantification of *lanes* in *A* without (*black bars*) and with (*white bars*) caffeine. 100% replication is defined as the signal in the 60-min lane. *C*, representative combed DNA fibers of sperm nuclei replicated in egg extracts (2000 nuclei/μl) in the absence or presence of 5 mM caffeine. Biotin-dUTP was added at 30 min (*bar*, 10 kb). *D*, average replication extent of combed DNA fibers at the indicated time points in the absence (*black bars*) or presence (*white bars*) of caffeine.

This was further explored by combing DNA from sperm nuclei (2000 nuclei/μl) replicated in the presence or absence of caffeine (Figs. 4*C* and 5*A*). Early in S phase (30 min) (Fig. 4, *C* and *D*), the replication extent was 2.3-fold higher in the presence of caffeine (19.6%) than in the control (9.5%). This resulted from shorter overall eye-to-eye distances (mean of 20.7 *versus* 37.2 kb) and only slightly longer eyes (mean of 4.1 *versus* 3.5 kb). These data agree well with the electrophoretic analysis of nascent strands described above. At 40 min, however, the difference in replication extent was reduced (55.2 *versus* 40.7%, respectively), and at 50 min it was abolished (84.7 *versus* 82.5%) (Fig. 4*D*). Thus, although caffeine initially increased the rate of DNA synthesis during early S phase, this rate slowed down later, so that no net effect of caffeine on S phase length was observed. Paradoxically, the fork density remained higher in the presence of caffeine throughout S phase (Fig. 5*B*). The increase in the frequency of initiation early in S phase resulted in a tighter spacing of clusters (mean excluded distance 42.2 kb *versus* 63.1 kb; 21 of 113 *versus* 42 of 127 unreplicated fibers) as well as a tighter spacing of eyes within clusters at 30 min (Fig. 5*C*, 12.0 *versus* 16.1 kb). Eye spacing remained tighter in the presence of caffeine than in the control at 40 min (13.1 *versus* 17.7 kb) and 50 min (26.8 *versus* 34.5 kb). A significant excess of distances in the 5–10-kb range was observed (Fig. 5*C*, and data not shown).

Despite an identical length of eyes at 40 min (7.2 kb), eyes grew from 40 to 50 min to a smaller size in the presence of caffeine (21.9 kb) than in the control (28.6 kb). This did not result from a different frequency of mergers, because eye spacing doubled in both cases. Instead, fork velocities were 25–50% lower throughout S phase in the presence of caffeine (25–30 min: 880 *versus* 670 nt·min^{-1}; 30–40 min: 370 *versus* 280 nt·min^{-1}; 40–50 min: 490 *versus* 230 nt·min^{-1}). Velocity partly recovered late in S phase in the control, as in some experiments above, but not in the caffeine sample (Fig. 5*C*). Furthermore, the mean gap length decreased much more slowly in the presence of caffeine (from 5.8 to 4.9 kb) than in the control (from 10.5 to 5.9 kb) from 40 to 50 min. Given the average fork

A

Incubation time	30 min		40 min		50 min	
Caffeine	-	+	-	+	-	+
Total DNA length (kb)	9938	7835	10739	11809	10710	8957
Total replicated length (kb)	942	1535	4373	6524	8890	7328
Replication extent	9.5%	19.6%	40.7%	55.2%	83.0%	81.8%
Total # of fibers	127	113	121	133	103	94
Unreplicated fibers	42	21	2	3	0	0
Fully replicated fibers	0	0	0	0	22	18
Mean fiber length (kb)	78.2	69.3	88.7	88.8	103.9	79.9
Total # of forks	534	758	1212	1808	621	668
fork density (forks/kb)	1/18.6	1/10.3	1/8.9	1/6.5	1/17.2	1/13.4
Eye-to-eye distances (kb) :						
overall	37.2	20.7	17.7	13.1	34.5	26.8
local: mean, (#)	16.1 (147)	12.0 (270)	13.9 (495)	11.9 (734)	18.0 (217)	15.5 (245)
excluded : mean, (#)	63.1 (120)	42.2 (109)	34.8 (111)	17.6 (175)	72.8 (93.5)	58.0 (89)
Eye lengths (kb) :						
overall	3.5	4.1	7.2	7.2	28.6	21.9
local : mean, (#)	3.5 (248)	4.1 (379)	7.2 (605)	7.2 (904)	14.6 (289)	13.8 (308)
excluded : mean, (#)	3.9 (19)	-	17.4 (1)	-	217.2 (21.5)	118.4 (26)
Gap lengths (kb) :						
overall	33.7	16.6	10.5	5.8	5.9	4.9
local : mean, (#)	11.6 (175)	7.7 (287)	6.7 (496)	4.5 (734)	5.1 (240)	3.8 (289)
excluded : mean, (#)	68.3 (102)	44.5 (92)	27.7 (110)	11.7 (170)	8.5 (70.5)	11.8 (45)

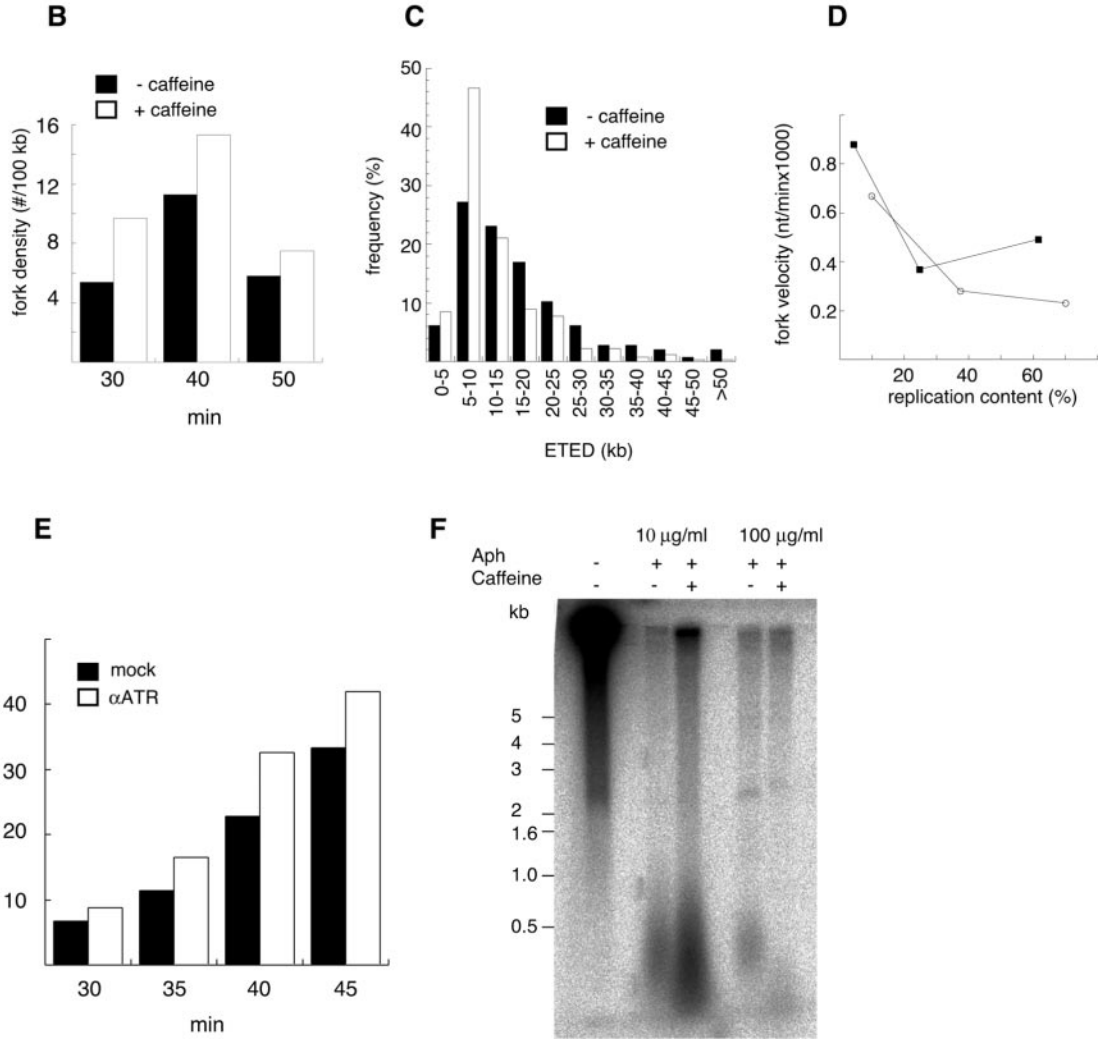

FIG. 5. **An intra-S phase checkpoint restrains initiation and promotes fork progression.** *A*, replication parameter values of combed DNA fibers for each successive time point at 2000 nuclei/μl in the presence or absence of caffeine. *B*, fork density in the absence (*black bars*) and presence of caffeine (*white bars*) at different time points. *C*, distribution of eye-to-eye distances (*ETED*) at 30 min in the absence (*black bars*) and presence of caffeine (*white bars*). *D*, fork velocities in the absence (*black squares*) and presence of caffeine (*white circles*) plotted against replication extent. *E*, nascent strand synthesis in the presence of ATR-neutralizing antibodies (*αATR*, *white bars*) or control rabbit anti-mouse antibodies (*mock*, *black bars*) was analyzed as described in the legend to Fig. 4, *A* and *B*. The experiment was repeated twice with very similar results. *F*, sperm nuclei (2000 nuclei/μl) were incubated in egg extracts in the presence of 0, 10, and 100 μg/ml aphidicolin (*Aph*) with 0 or 5 mM caffeine as indicated for 2 h, and nascent DNA strands were analyzed by alkaline gel electrophoresis.

velocity at that time (230 nt·min^{-1}), these results suggest that a significant fraction of the forks may be stalled in the caffeine-treated extract.

We conclude that initiation during unchallenged S phase is under control of a caffeine-sensitive checkpoint in *Xenopus* egg extracts. This control is tighter at high nuclei concentration,

suggesting that titration of some factor increases the checkpoint signal. Abrogation of this control by caffeine results in increased initiation and abnormal slowing or stalling of some forks late in S phase. Similar effects of caffeine were observed at 6000 nuclei/μl (not shown).

We checked whether these effects were also observed when nuclei released from a replication block with aphidicolin alone were transferred into fresh extract with or without caffeine. At 7 min, the replication content was 2-fold higher in the presence of caffeine (14.6%) than in the control (7.5%) due to shorter eye-to-eye distances (overall, 30.6 *versus* 48.6 kb) and slightly longer eyes (4.4 *versus* 3.6 kb). Cluster spacing was tighter (10 of 56 *versus* 23 of 67 unreplicated fibers), but eye spacing within clusters was similar (20.5 *versus* 20.9 kb). At 15 min, the difference in replication extent was reduced (27.9 *versus* 21.3%), and eye spacing was similar (overall, 24.1 *versus* 25.8 kb). Fork velocities were low and similar without or with caffeine (0–7 min: 260 *versus* 320 nt·min^{-1}; 7–15 min: 290 *versus* 220 nt·min^{-1}). These results verify that replication forks progress slowly after aphidicolin release and indicate that this is not reversed by checkpoint abrogation. These results also corroborate that caffeine increases initiation early in S phase.

Caffeine is an inhibitor of ATM and ATR checkpoint kinases. Whereas ATM is activated by DNA double strand breaks, ATR chromatin binding and activity are enhanced by stalled replication forks (36). Furthermore, ATR associates with chromatin during unperturbed DNA replication in *Xenopus* (37). To examine whether ATR controls origin firing during unperturbed S phase, we analyzed the effect of ATR-neutralizing antibodies (34) on nascent strand synthesis by alkaline-agarose gel electrophoresis. As observed before with caffeine (Fig. 4, *A* and *B*), the addition of ATR-neutralizing antibodies increased the rate of nascent strand synthesis early in S phase (Fig. 5*E*), albeit to a lower extent (~1.4-fold). Since nascent strand size profile was unchanged, we conclude that ATR inhibition increased origin firing. This result suggests that the origin-firing checkpoint that operates during unperturbed S phase is at least in part dependent on ATR (see "Discussion").

We were intrigued to know whether this checkpoint is identical to the one that blocks origin firing in response to aphidicolin. In a previous work (15), we failed to observe an effect of caffeine on the block to origin firing triggered by a high concentration of aphidicolin (100 μg/ml). Here we incubated sperm nuclei in the presence of 0, 10, or 100 μg/ml aphidicolin and [α-^{32}P]dATP with or without caffeine and analyzed the nascent strands formed after 2 h using alkaline gel electrophoresis (Fig. 5*F*). Small (<1 kb) nascent strands accumulated at both concentrations of aphidicolin alone, although in lower amounts at 100 than at 10 μg/ml. We observed that caffeine increased the accumulation of small nascent strands ~3-fold at 10 μg/ml aphidicolin. In contrast, caffeine did not increase the accumulation of nascent strands at 100 μg/ml aphidicolin, as reported previously (15). The nascent strand size at 100 μg/ml aphidicolin was smaller in the presence of caffeine, but this was not reproduced in other experiments. These results suggest that initiation is still under control of a caffeine-sensitive checkpoint at 10 μg/ml aphidicolin. The stronger inhibition of DNA synthesis by 100 μg/ml aphidicolin may render a stimulation of initiation by caffeine more difficult to detect, especially if stalled nascent strands are destabilized in the absence of a checkpoint. Alternatively, this higher concentration of aphidicolin may elicit a different or additional caffeine-insensitive checkpoint that further blocks initiation.

DISCUSSION

We have investigated what regulates origin firing timing and S phase length in *Xenopus* egg extract. This reveals that the replication program can be modulated by the nucleocytoplasmic ratio and the checkpoint inhibitor, caffeine. At all concentrations of nuclei, origins are activated in clusters that fire at different times. Increasing the concentration of nuclei in the extract (i) does not markedly alter origin spacing, (ii) spreads the time over which distinct clusters undergo activation, and (iii) slows the progression of replication forks. The latter two effects explain why S phase is longer at high concentration of nuclei. Caffeine abrogates the spreading of origin firing time, especially at high nuclei concentration. Therefore, a caffeine-sensitive checkpoint that responds to the nucleocytoplasmic ratio, in the absence of replication inhibitors or DNA-damaging agents, controls the time at which different origin clusters fire. However, caffeine does not increase fork velocity and actually causes at least some forks to slow or stall late in S phase. ATR inhibition with specific antibodies has similar effects to caffeine on origin firing, implying a role for ATR in an origin-firing checkpoint during unperturbed S phase.

Origin Clusters—The tendency to be grouped into synchronous clusters is a general feature of eukaryotic replication origins (38). The *Xenopus* clusters contain 5–8 origins and span 50–100 kb (17). Here we show this organization is found at all concentrations of nuclei, but different clusters fire over a compressed time frame at low concentration. This was not apparent when the correlation between the length of adjacent eyes was calculated, since it did not significantly change with nuclei concentration (0.16–0.22). This is because eyes of >8 kb and replicons not yet fired are not taken into account by this approach. In contrast, the distribution of eye number per fiber takes into account all DNA fibers. Our double-labeling and combing protocol detects all fibers irrespective of the number or aspect of replication eyes, which proved essential to demonstrate this point.

The relative synchrony of origin firing within a cluster may be explained in two ways. First, some event distinct from origin firing (*e.g.* chromatin remodeling of a 50–100-kb DNA segment), may suddenly increase the probability of initiation within that segment. Second, the firing of a first origin may increase the probability of nearby (50–100 kb) initiation (positive interference). We suggest that tethering a first potential origin to a replication factory facilitates the subsequent attachment of nearby origins to the same factory (positive interference). However, attachment of too closely spaced origins (<5–10 kb) would be disfavored by the high bending energy of short DNA loops (negative interference (13)). Measurements of the flexibility of chromatin fibers suggest an optimal loop size of ~10 kb (39). Thus, multipoint attachment of a 50–100-kb DNA segment to a single replication factory may explain both the observed range of replicon sizes and the relative synchrony of adjacent origins (40).

The Intra-S Checkpoint Regulates Origin Firing in the Absence of DNA-damaging Agents or DNA Replication Inhibitors—We confirm that increasing the concentration of nuclei in an egg extract lengthens S phase (29). Walter and Newport (29) reported that this only occurs above a threshold concentration of 2000 nuclei/μl, whereas we already find a significant difference between 100 and 2000 nuclei/μl. This superficial discrepancy could be explained by differences in extract preparation or by the fact that Walter and Newport used Ara-C to synchronize nuclei. A reaction containing 2000 haploid nuclei/μl corresponds to an embryo containing ~600 diploid cells, whereas the MBT only occurs at the 4000–8000-cell stage. In *Drosophila*, S phase begins to slow down several cell cycles before the MBT occurs, so this could be happening in *Xenopus* as well.

Walter and Newport (29) suggested that S phase lengthens because some factor that controls replicon size becomes stoi-

chiometrically limiting. Several observations conflict with this model. First, initiation can be considerably accelerated by caffeine, at least early in S phase. Second, the maximal density of forks is the same at all nuclear concentrations and can be increased by caffeine. Clearly, more initiation and elongation factors are available than are actually used during normal S phase. Third, we demonstrate that increasing the nucleocytoplasmic ratio spreads the time during which different origin clusters fire but does not markedly alter interorigin distance within clusters. However, the time it takes to reach the maximal fork density does increase at high nuclei concentration. At high concentration, nuclei may kinetically compete for import of some replication factor(s), although the same amount of factor(s) per nucleus may be imported given sufficient time.

We suggest that the caffeine-sensitive checkpoint, rather than responding to the exhaustion of a replication factor, senses when its concentration becomes too low for optimal chromosomal replication. Consistently, forks slow down at high nuclei concentration and during S phase progression, when fork density increases. This is not reverted by caffeine, suggesting that slowing occurs upstream of checkpoint activation. In fact, forks further slow down or even stall in the presence of caffeine. This may result from some checkpoint-independent effect of caffeine. However, replication forks also slow down anomalously during unchallenged S phase in budding yeast *mec1* mutants (41). It was proposed that Mec1 monitors development of regular chromosomal structure behind the forks and promotes their progression through specific zones accordingly. Our results could reflect an analogous role for ATM or ATR in *Xenopus*. Alternatively, fork slowing in caffeine-treated egg extracts may result from deregulated origin firing and assembly of an excessive number of forks, in conditions where the concentration of some fork component is not optimal.

The checkpoint may also monitor the number of active forks so as to control further initiation in unchallenged S phase. The maximal fork density is independent of nuclear concentration but can be increased by caffeine treatment. Caffeine inhibits both ATM and ATR *in vitro* (30). ATM is activated in response to DNA double strand breaks, whereas ATR in complex with its partner ATRIP responds to extended regions of RPA-single-stranded DNA generated at stalled replication forks (36). Although only a low level of RPA-single-stranded DNA is associated with unperturbed replication forks, ATR associates with chromatin during unperturbed DNA replication in *Xenopus* (37). We speculate that the gradual increase in fork density early in S phase activates ATR to reduce origin firing and optimize fork density. Our observation that ATR-neutralizing antibodies increase origin firing in otherwise unpertubed S phase supports this model. Recent work suggests that a caffeine-sensitive, Chk1-dependent checkpoint also regulates mouse and SV40 virus origins in the absence of DNA damage (42). Down-regulation of either Cdc7/Dbf4 or Cdk2-cyclin E kinases following ATR/Chk1 activation could mediate checkpoint inhibition of origin firing (43, 44). However, the fact that ATR-neutralizing antibodies increase origin firing to a lower extent than caffeine suggests that ATM and/or other pathways also might be involved.

Caffeine effects are not limited to ATM/ATR. In certain mammalian cells, caffeine abrogates checkpoints even under conditions where it fails to inhibit ATM/ATR *in vivo*, and it appears to do so by interfering with signaling downstream of ATM/ATR (31, 32). In *Xenopus* egg extracts, however, caffeine does inhibit ATR-dependent phosphorylation events (34). Another notable target of caffeine is the phosphodiesterase/cyclic AMP pathway (45). However, we found that 3-isobutyl-1-methylxanthine, a nonspecific phosphodiesterase inhibitor (46), does not increase the rate of nascent strand synthesis in egg extracts (data not shown). Thus, the stimulatory effect of caffeine on origin firing is unlikely to be due to phosphodiesterase inhibition.

Walter and Newport (29) found that adding the cyclin-dependent kinase inhibitor p21 (Cip1) to nuclei released from Ara-C arrest had little effect on subsequent DNA synthesis. However, a significant effect of p21 addition to nuclei released from aphidicolin was reported elsewhere (47), consistent with cyclin-dependent kinase-dependent late initiation. We have examined by DNA combing the effect of adding the Cdk2 inhibitors p27 (Kip1) or roscovitine to nuclei released from aphidicolin (data not shown). A decrease in replication rate and fork density was indeed observed. However, small bubbles still appeared throughout S phase, suggesting incomplete inhibition of late origins. This perhaps explains why Walter and Newport did not observe a stronger effect of Cip1 inhibition.

In summary, we conclude that an intra-S phase checkpoint controls the time of origin firing in *Xenopus* egg extracts, an early embryonic system where replication timing is disconnected from gene expression and sequence-specific initiation. The replication patterns observed here can be explained simply assuming that (i) abundant potential origins are activated at an increasing frequency as S phase progresses; (ii) negative and positive origin interference modulate the probability of initiation over characteristic distances (<5–10 and 50–100 kb, respectively), resulting in cluster organization of replication eyes; and (iii) the frequency of initiation is under control of a caffeine-sensitive, ATR-dependent checkpoint. Thus, there is no need to postulate a differential marking of early and late replicating domains in this system. We suggest that the checkpoint adjusts the frequency of initiation, and therefore the rate of DNA synthesis, by responding in complementary ways to available replication fork components and active replication forks throughout S phase. Further work is needed to define the sensors and effectors of the checkpoint and to decipher how the connection between replication timing and epigenetic states of chromatin and transcription (25, 26) is, later in development, implemented on this elementary replication timing device.

Acknowledgments—We thank J.-F. Allemand, B. Berge, Z. Gueroui, and C. Place for coverslips; P. Lupardus and K. Cimprich for the anti-ATR antibodies; and J. Huberman, J. Walter, G. Pierron, and the laboratory members for critical reading of the manuscript.

REFERENCES

1. Bell, S. P., and Dutta, A. (2002) *Annu. Rev. Biochem.* **71,** 333–374
2. Romanowski, P., Madine, M. A., Rowles, A., Blow, J. J., and Laskey, R. A. (1996) *Curr. Biol.* **6,** 1416–1425
3. Coleman, T. R., Carpenter, P. B., and Dunphy, W. G. (1996) *Cell* **87,** 53–63
4. Rowles, A., Chong, J. P., Brown, L., Howell, M., Evan, G. I., and Blow, J. J. (1996) *Cell* **87,** 287–296
5. Maiorano, D., Moreau, J., and Mechali, M. (2000) *Nature* **404,** 622–625
6. Walter, J., and Newport, J. (2000) *Mol. Cell* **5,** 617–627
7. Kubota, Y., Takase, Y., Komori, Y., Hashimoto, Y., Arata, T., Kamimura, Y., Araki, H., and Takisawa, H. (2003) *Genes Dev.* **17,** 1141–1152
8. Hyrien, O., and Méchali, M. (1993) *EMBO J.* **12,** 4511–4520
9. Hyrien, O., Maric, C., and Méchali, M. (1995) *Science* **270,** 994–997
10. Maric, C., Levacher, B., and Hyrien, O. (1999) *J. Mol. Biol.* **291,** 775–788
11. Newport, J., and Kirschner, M. (1982) *Cell* **30,** 675–686
12. Laskey, R. A. (1985) *J. Embryol. Exp. Morphol.* **89,** (suppl.) 285–296
13. Lucas, I., Chevrier-Miller, M., Sogo, J. M., and Hyrien, O. (2000) *J. Mol. Biol.* **296,** 769–786
14. Herrick, J., Stanislawski, P., Hyrien, O., and Bensimon, A. (2000) *J. Mol. Biol.* **300,** 1133–1142
15. Marheineke, K., and Hyrien, O. (2001) *J. Biol. Chem.* **276,** 17092–17100
16. Hyrien, O., Marheineke, K., and Goldar, A. (2003) *BioEssays* **25,** 116–125
17. Blow, J. J., Gillespie, P. J., Francis, D., and Jackson, D. A. (2001) *J. Cell Biol.* **152,** 15–26
18. Edwards, M. C., Tutter, A. V., Cvetic, C., Gilbert, C. H., Prokhorova, T. A., and Walter, J. C. (2002) *J. Biol. Chem.* **277,** 33049–33057
19. Harvey, K. J., and Newport, J. (2003) *Mol. Cell. Biol.* **23,** 6769–6779
20. Raghuraman, M. K., Brewer, B. J., and Fangman, W. L. (1997) *Science* **276,** 806–809
21. Donaldson, A. D., Raghuraman, M. K., Friedman, K. L., Cross, F. R., Brewer, B. J., and Fangman, W. L. (1998) *Mol. Cell* **2,** 173–182
22. Santocanale, C., and Diffley, J. F. (1998) *Nature* **395,** 615–618

23. Shirahige, K., Hori, Y., Shiraishi, K., Yamashita, M., Takahashi, K., Obuse, C., Tsurimoto, T., and Yoshikawa, H. (1998) *Nature* **395,** 618–621
24. Sharma, K., Weinberger, M., and Huberman, J. A. (2001) *Genetics* **159,** 35–45
25. Goren, A., and Cedar, H. (2003) *Nat. Rev. Mol. Cell. Biol.* **4,** 25–32
26. McNairn, A. J., and Gilbert, D. M. (2003) *BioEssays* **25,** 647–656
27. Dimitrova, D. S., and Gilbert, D. M. (1999) *Mol. Cell* **4,** 983–993
28. Dimitrova, D. S., and Gilbert, D. M. (2000) *Nat. Cell Biol.* **2,** 686–694
29. Walter, J., and Newport, J. W. (1997) *Science* **275,** 993–995
30. Sarkaria, J. N., Busby, E. C., Tibbetts, R. S., Roos, P., Taya, Y., Karnitz, L. M., and Abraham, R. T. (1999) *Cancer Res.* **59,** 4375–4382
31. Cortez, D. (2003) *J. Biol. Chem.* **278,** 37139–37145
32. Kaufmann, W. K., Heffernan, T. P., Beaulieu, L. M., Doherty, S., Frank, A. R., Zhou, Y., Bryant, M. F., Zhou, T., Luche, D. D., Noikolaishvilli-Feinberg, N., Simpson, D. A., and Cordeiro-Stone, M. (2003) *Mutat Res.* **532,** 85–102
33. Blow, J. J., and Laskey, R. A. (1986) *Cell* **47,** 577–587
34. Lupardus, P. J., Byun, T., Yee, M. C., Hekmat-Nejad, M., and Cimprich, K. A. (2002) *Genes Dev.* **16,** 2327–2332
35. Michalet, X., Ekong, R., Fougerousse, F., Rousseaux, S., Schurra, C., Hornigold, N., van Slegtenhorst, M., Wolfe, J., Povey, S., Beckmann, J. S., and Bensimon, A. (1997) *Science* **277,** 1518–1523
36. Zou, L., and Elledge, S. J. (2003) *Science* **300,** 1542–1548
37. Hekmat-Nejad, M., You, Z., Yee, M. C., Newport, J. W., and Cimprich, K. A. (2000) *Curr. Biol.* **10,** 1565–1573
38. Berezney, R., Dubey, D. D., and Huberman, J. A. (2000) *Chromosoma* **108,** 471–484
39. Rippe, K. (2001) *Trends Biochem. Sci.* **26,** 733–740
40. Jun, S., Herrick, J., Bensimon, A., and Bechhoefer, J. (2004) *Cell Cycle* **3,** 223–229
41. Cha, R. S., and Kleckner, N. (2002) *Science* **297,** 602–606
42. Miao, H., Seiler, J. A., and Burhans, W. C. (2003) *J. Biol. Chem.* **278,** 4295–4304
43. Costanzo, V., Robertson, K., Ying, C. Y., Kim, E., Avvedimento, E., Gottesman, M., Grieco, D., and Gautier, J. (2000) *Mol. Cell* **6,** 649–659
44. Costanzo, V., Shechter, D., Lupardus, P. J., Cimprich, K. A., Gottesman, M., and Gautier, J. (2003) *Mol. Cell* **11,** 203–213
45. Fredholm, B. B., Battig, K., Holmen, J., Nehlig, A., and Zvartau, E. E. (1999) *Pharmacol. Rev.* **51,** 83–133
46. Choi, O. H., Shamim, M. T., Padgett, W. L., and Daly, J. W. (1988) *Life Sci.* **43,** 387–398
47. Strausfeld, U. P., Howell, M., Rempel, R., Maller, J. L., Hunt, T., and Blow, J. J. (1994) *Curr. Biol.* **4,** 876–883